

THERMAL DECOMPOSITION KINETICS OF THE SYNTHETIC COMPLEX Pb(1,4-BDC)·(DMF)(H₂O)

J. Zhang^{1,2}, J. L. Zeng^{1,2}, Y. Y. Liu^{1,2}, L. X. Sun^{1*}, F. Xu¹, W. S. You³ and Y. Sawada⁴

¹Materials and Thermochemistry Laboratory, Dalian Institute of Chemical Physics, Chinese Academy of Sciences Dalian 116023, P.R. China

²Graduate School of the Chinese Academy of Sciences, Beijing 100049, P.R. China

³Liaoning Normal Univ., Fac. Chem. and Chem. Engr., Dalian 116029, P.R. China

⁴Department of Nanochemistry, Faculty of Engineering, Tokyo Polytechnic University, 1583 Iiyama, Atsugi, Kanagawa, 243-0297 Japan

Pb(1,4-BDC)·(DMF)(H₂O) (1,4-BDC=1,4-benzenedicarboxylate; DMF=dimethylformamide) has been synthesized and investigated by elemental analysis, FTIR spectroscopy, thermogravimetry (TG), derivative thermogravimetry (DTG). TG-DTG curves show that the thermal decomposition occurs in four stages and the corresponding apparent activation energies were calculated with the Ozawa–Flynn–Wall (OFW) and the Friedman methods. The most probable kinetic model function of the dehydration reaction of the compound has been estimated by the Coats–Redfern integral and the Achar–Bridly–Sharp differential methods in this study.

Keywords: apparent activation energy, kinetic model, TG-DTG, thermal decomposition

Introduction

1,4-benzenedicarboxylic acid (1,4-H₂BDC) with a 180° separation between the two carboxylic groups can be coordinated with many transition and non-transition metals, which is an ideal ligand to design novel coordination polymers and metal organic open framework structures [1–4]. A series of transition-metal complexes with 1,4-benzenedicarboxylate (1,4-BDC) and its derivatives have been reported and investigated due to their potential applications in separations, hydrogen sorption, non-linear optics, magnetism and catalysis [4–8]. In contrast to other transition-metal 1,4-benzenedicarboxylate complexes, lead complexes with 1,4-BDC are much less studied. Recently, Yaghi *et al.* reported Pb(1,4-BDC)(C₂H₅OH)·(C₂H₅OH), which becomes unstable exposure to air [4]. In addition, some thermal behaviors of metal complexes have been already investigated by a number of researchers [9–11], but there has been very little report on thermal decomposition kinetics in literature up to now. Kinetic analysis of thermal analysis data is an important tool for estimating the thermal stability and allows obtaining some information on thermal decomposition mechanisms at high temperature.

In the present work, Pb(1,4-BDC)·(DMF)(H₂O) (DMF=dimethylformamide) has been synthesized and characterized by elemental analysis, FTIR spectroscopy and thermogravimetric (TG) analysis. Kinetic methods, such as the Ozawa–Flynn–Wall (OFW) [12, 13] and

Friedman [14] were used in this study to evaluate the apparent activation energy. The most probable kinetic model of thermal dehydration of the compound has been suggested according to Coats–Redfern integral method and Achar–Bridly–Sharp differential method.

Experimental

Sample preparation

All materials were commercially available and were of analytical grade unless stated elsewhere. The lead complex was synthesized using solvothermal method. Lead(II) nitrate (1.66 g, 5.0 mmol) and 1,4-H₂BDC (0.83 g, 5.0 mmol) were dissolved in DMF/1,4-dioxane (5:2 by volume, 70 mL). The clear solution was then removed in a Teflon bomb. The bomb was heated to 393 K and maintained at this temperature for 3 days. After slowly cooling down to the room temperature, the final product obtained as yellowish crystals was collected by filtration and washed three times with DMF (50 mL) and dried in air. This lead complex is air stable and is insoluble in water and most of the common organic solvents.

Elemental analyses for C₁₁H₁₃NO₆Pb found (%): C, 28.58; H, 2.24; N, 3.16; calc. (%): C, 28.55; H, 2.81; N, 3.03. The content of lead was determined by thermogravimetry analysis. The purity of the sample was >99.0%.

* Author for correspondence: lxsun@dicp.ac.cn

FTIR (KBr pellet, 4000–400 cm⁻¹): 3450(br), 3049(w), 2929(w), 2881(w), 1645(s), 1547(s), 1500(w), 1437(w), 11371(s), 1315(w), 1296(w), 1256(w), 11460(w), 1103(m), 1063(w), 1016(m), 982(w), 885(m), 864(w), 835(w), 746(s), 660(m), 519(s), 410(w). FTIR spectroscopy shows that the carboxyl groups of the ligand have been coordinated to the metal ion.

Methods

Elemental analysis was carried on PE-2400 II Series CHNS/O analyzer. FTIR spectrum was recorded on Bruker Equinox 55 infrared spectrometer using KBr pellet in the range of 4000–400 cm⁻¹.

Thermal analysis

A thermogravimetric analyzer (Model: Setsys 16/18, Setaram Co., France) was used for TG measurement of this sample under nitrogen atmosphere (99.999%). Several experiments were carried out at heating rates of $\beta=5, 10, 15, 20$ K min⁻¹ and the flow rate of nitrogen was 45 cm³ min⁻¹. The mass of the sample was ca. 10 mg. Two Al₂O₃ crucibles were used (capacity: 100 μ L). The reference crucible was filled with α -Al₂O₃. The TG equipment was calibrated by the CaC₂O₄·H₂O (99.9%).

Results and discussion

Thermal analysis

Figure 1 displays the TG and DTG curves obtained at heating rate of 5 K min⁻¹ under nitrogen atmosphere. The curves exhibit that the non-isothermal decomposition of the compound undergoes four stages in the temperature range of 300 to 900 K. The first mass loss starts at about 363 K and is about 3.83%

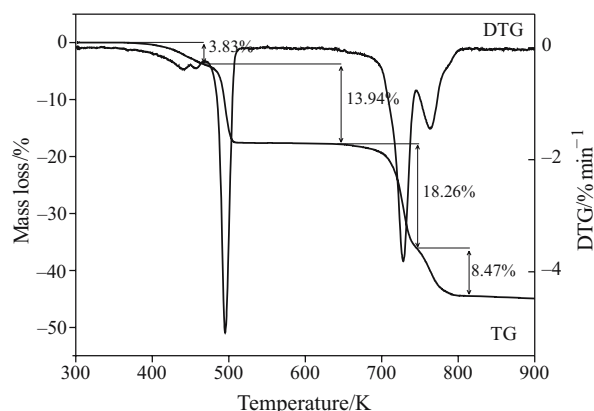
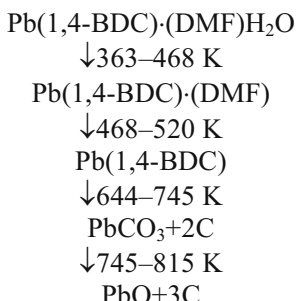


Fig. 1 TG-DTG curves of Pb(1,4-BDC)-(DMF)(H₂O) under high purity nitrogen atmosphere at heating rate of 5 K min⁻¹

(calcd. 3.89%) likely due to the loss of a molecule of water. The second stage takes place between 468 and 644 K and is accompanied by 13.94% mass loss which roughly coincides with the calculated value of 15.81%. It is attributed to the loss of a molecule of DMF. Subsequently, the decomposition of the ligand (1,4-BDC) is followed. Two well-separated peaks are presented on the DTG curve, this indicates that the decomposition of the ligand (1,4-BDC) is divided into two steps. The third rapid loss of 18.26% (calcd. 17.33%) and the fourth slow loss of 8.47% (calcd. 6.92%) are observed in the region of 644–815 K, and there is probably some complex of lead carbonate and carbon between the two processes (PbCO₃·2C). The overall mass loss of the sample is about 44.50% in accord with the calculated percentage (43.95%). Heating the black residue in air on an electric stove, the sample mass lost and the color became yellow. So the final black residue was estimated as inorganic mixture of lead monoxide and carbon under nitrogen atmosphere.

The possible mechanism of the thermal decompositions was deduced as follows:



Kinetic methods

Model-free estimation of activation energy

Two typical isoconversional methods of integral Ozawa–Flynn–Wall and differential Friedman have been widely applied to estimate the apparent activation energy without having to presuppose a certain kinetic model. Figure 2 shows the TG curves of Pb(1,4-BDC)-(DMF)(H₂O) measured in N₂ atmosphere from 300 to 900 K with the heating rate of 5, 10, 15, 20 K min⁻¹, respectively. The basic data (β , α , T) taken from the TG curves are used in the following equations:

Ozawa–Flynn–Wall equation [12, 13]:

$$\ln \beta = \ln \left(\frac{AE_a}{R} \right) - \ln g(\alpha) - 5.3305 - \frac{1.052E_a}{RT_a} \quad (1)$$

where β is heating rate, α extent of conversion, $g(\alpha)$ integral expression of kinetic function, E apparent activation energy, A pre-exponential factor and R gas

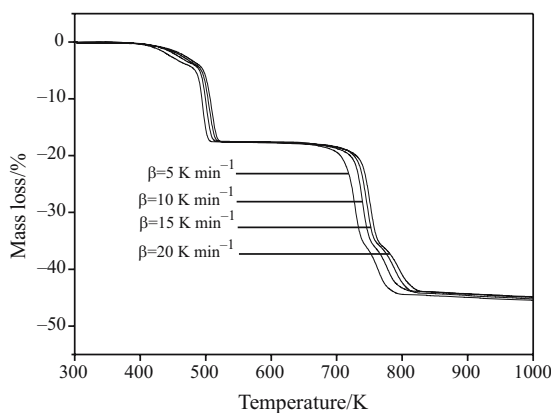


Fig. 2 TG curves of Pb(1,4-BDC)·(DMF)(H₂O) under high purity nitrogen atmosphere at 5, 10, 15, 20 K min⁻¹

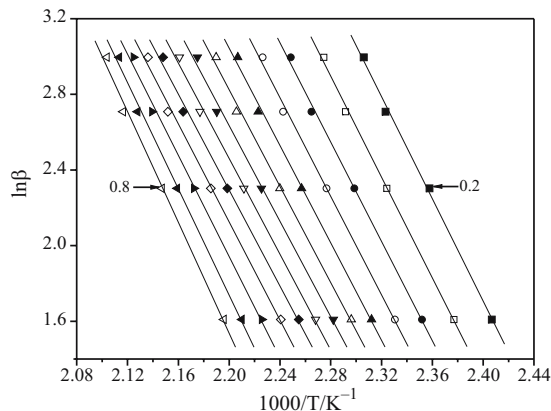


Fig. 3 OFW analysis of the thermal decomposition of Pb(1,4-BDC)·(DMF)(H₂O) for the first step at 5, 10, 15, 20 K min⁻¹

constant. The subscript α indicates the values related to a particular extent of conversion. For constant values of α , plots of $\ln\beta$ vs. $1/T_\alpha$ should fit to a straight line with a slope of $-1.052E_a/R$. Such plots for the dehydration step of the complex at different α ($0.2 \leq \alpha \leq 0.8$) are exhibited in Fig. 3.

Friedman equation [14]:

$$\ln\left(\frac{d\alpha}{dt}\right)_a = \ln[Af(\alpha)] - \frac{E_a}{RT_\alpha} \quad (2)$$

where $d\alpha/dt$ is the rate of conversion and $f(\alpha)$ differential expression of kinetic function. A plot of $\ln(d\alpha/dt)_a$ vs. $1/T_\alpha$ gives a straight line with a slope of $-E_a/R$.

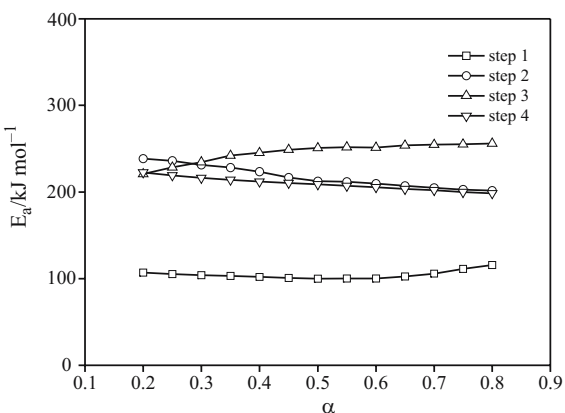


Fig. 4 Apparent activation energy in relation to the conversion for the four steps based on the OFW method

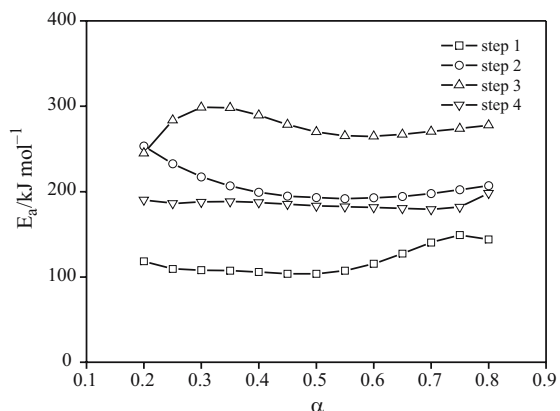


Fig. 5 Apparent activation energy in relation to the conversion for the four steps based on the Friedman method

For four decomposition stages, the apparent activation energy can be calculated at different extent of conversion (in the range $0.2 \leq \alpha \leq 0.8$) using both Eqs (1) and (2), and the results are presented in Figs 4 and 5, respectively. The average value and standard deviation of the activation energies are tabulated in Table 1.

Comparing the results from two isoconversional methods, the apparent activation energies values calculated by Friedman method are larger than those of OFW method for the first and third steps. However, the reverse results are obtained for the other steps. It is well known that Friedman method is very sensitive to experimental noise, and tends to be numerically unstable because of employing instantaneous rate value. But OFW method produces a systematic error in E_a .

Table 1 Apparent activation energy obtained from the OFW and Friedman methods for four steps

Method	$E_a/kJ mol^{-1}$			
	step 1	step 2	step 3	step 4
OFW	104.42±4.70	217.27±12.82	245.66±11.19	209.24±7.42
Friedman	118.46±16.33	206.29±18.33	275.62±14.73	185.53±5.03

when the activation energy varies with α . This error does not appear in Friedman method [15].

Determination of the most probable kinetic model

Coats–Redfern integral equation [16, 17]

$$\ln \frac{g(\alpha)}{T^2} = \ln \frac{AR}{\beta E} - \frac{E}{RT} \quad (3)$$

The values of E , $\ln A$ and the linear correlation coefficients r are calculated from the linear least-squares plot of $\ln[g(\alpha)/T^2]$ vs. $1/T$, which the slope is equal to $-E/R$ and the intercept is equal to $\ln(AR/\beta E)$.

Achar–Brindly–Sharp differential equation [18]

$$\ln \left[\frac{1}{f(\alpha)} \frac{d\alpha}{dt} \right] = \ln(A/\beta) - \frac{E}{RT} \quad (4)$$

Plotting $\ln\{[1/f(\alpha)][d\alpha/dt]\}$ vs. $1/T$, a straight line is given. The activation energy E and pre-exponential factor A can be obtained from the slope $-E/R$ and the intercept $\ln(A/\beta)$.

The basic data α , T and $d\alpha/dt$ of the four decomposition steps and fifteen reaction models commonly used in solid-state reaction kinetics [19] were inserted into Eqs (3) and (4).

For the first step of dehydration, the results and the reaction model are listed in Table 2. Comparing the activation energies data in Tables 1 and 2, the possible

Table 2 Non-isothermal kinetic parameters obtained from Coats–Redfern equation and Achar–Brindley–Sharp equation for $\beta=5 \text{ K min}^{-1}$ for the first step

Mechanism	Achar–Brindley–Sharp				Coats–Redfern			
	$E/\text{kJ mol}^{-1}$	$\ln A/\text{s}^{-1}$	r	SD	$E/\text{kJ mol}^{-1}$	$\ln A/\text{s}^{-1}$	r	SD
A2	38.75	8.41	-0.9767	0.0632	32.15	6.35	-0.9994	0.0082
A3	25.62	4.46	-0.9481	0.0638	19.03	2.28	-0.9993	0.0053
A4	19.05	2.40	-0.9108	0.0641	12.46	0.09	-0.9991	0.0039
D1	82.80	20.18	-0.9701	0.1537	105.34	26.35	-0.9972	0.0588
D2	105.28	26.02	-0.9886	0.1189	118.27	29.55	-0.9988	0.0425
D3	131.46	32.11	-0.9967	0.0797	133.85	32.70	-0.9997	0.0250
D4	114.26	27.12	-0.9926	0.1038	123.42	29.59	-0.9993	0.0353
F1	78.13	19.73	-0.9943	0.0624	71.54	17.78	-0.9995	0.0168
F2	129.74	34.71	-0.9933	0.1120	100.67	26.56	-0.9949	0.0758
PL2	-1.63	-3.30	0.1035	0.1161	20.91	2.65	-0.9953	0.0151
PL3	-11.01	-6.16	0.5885	0.1122	11.53	-0.40	-0.9929	0.0103
PL4	-15.70	-7.67	0.7262	0.1103	6.84	-2.15	-0.9882	0.0079
R1	26.52	4.76	-0.8377	0.1282	49.06	10.86	-0.9967	0.0297
R2	52.32	11.55	-0.9760	0.0867	59.47	13.40	-0.9993	0.0160
R3	60.92	13.64	-0.9863	0.0756	63.31	14.17	-0.9996	0.0126

Table 3 The kinetics parameters from differential method and integral method for the possible four kinetic models at the four heating rates for the first step

Heating rate/ K min^{-1}	Model	Achar–Brindley–Sharp			Coats–Redfern		
		$E/\text{kJ mol}^{-1}$	$\ln A/\text{s}^{-1}$	r	$E/\text{kJ mol}^{-1}$	$\ln A/\text{s}^{-1}$	r
5	D2	105.28	26.02	-0.9886	118.27	29.55	-0.9988
	D3	131.46	32.11	-0.9967	133.85	32.70	-0.9997
	D4	114.26	27.12	-0.9926	123.42	29.59	-0.9993
	F2	129.74	34.71	-0.9933	100.67	26.56	-0.9949
10	D2	114.44	28.52	-0.9975	117.39	28.49	-0.9999
	D3	139.76	34.21	-0.9993	132.50	31.40	-0.9995
	D4	123.12	29.48	-0.9988	122.39	28.45	-0.9999
	F2	136.38	36.36	-0.9885	98.64	25.28	-0.9904
15	D2	118.51	29.59	-0.9996	117.61	28.04	-0.9999
	D3	143.69	35.13	-0.9980	132.63	30.88	-0.9990
	D4	127.14	30.50	-0.9994	122.58	27.98	-0.9997
	F2	139.81	37.17	-0.9808	98.43	24.80	-0.9878
20	D2	122.59	30.77	-0.9992	119.22	28.24	-0.9999
	D3	147.77	36.26	-0.9964	134.27	31.05	-0.9988
	D4	131.22	31.66	-0.9984	124.20	28.17	-0.9996
	F2	143.09	38.08	-0.9769	99.21	24.80	-0.9871

four kinetic models and respective kinetic parameters at various heating rates are tabulated in Table 3.

From Table 3, we can see that function D4 (G-B equation), namely, $f(\alpha)=(3/2)[(1-\alpha)^{-1/3}-1]^{-1}$ and $g(\alpha)=1-2/3\alpha-(1-\alpha)^{2/3}$, is the most probable mechanism function of the dehydration of Pb(1,4-BDC)·(DMF)H₂O.

However, no reasonable kinetic model can be obtained for other three steps by means of above model-fitting methods. The results suggest that these three steps could not be interpreted by the fifteen reaction models in this study, or every single thermal decomposition step of them could be multi-step kinetics [20].

Acknowledgements

The authors gratefully acknowledge the National Nature Science Foundation of China for financial support to this work under Grant No. 20473091, 20573112 and 50671098.

References

- 1 H. Li, M. Eddaoudi, M. O'Keeffe and O. M. Yaghi, *Nature*, 402 (1999) 276.
- 2 O. M. Yaghi, M. O'Keeffe, N. W. Ockwig, H. K. Chae, M. Eddaoudi and J. Kim, *Nature*, 423 (2003) 705.
- 3 R. D. Poulsen, A. Bentien, M. Chevalier and B. B. Iversen, *J. Am. Chem. Soc.*, 127 (2005) 9156.
- 4 N. L. Rosi, J. Kim, M. Eddaoudi, B. Chen, M. O'Keeffe and O. M. Yaghi, *J. Am. Chem. Soc.*, 127 (2005) 1504.
- 5 H. J. Choi, T. S. Lee and M. P. Suh, *Angew. Chem. Int. Ed.*, 38 (1999) 1405.
- 6 J. S. Seo, D. M. Whang, H.-Y. Lee, S. I. Jun, J. H. Oh, Y. J. Jeon and K. M. Kim, *Nature*, 404 (2000) 982.
- 7 T. Sawaki and Y. Aoyama, *J. Am. Chem. Soc.*, 121 (1999) 4793.
- 8 S. Kitagawa, R. Kitaura and S. Noro, *Angew. Chem. Int. Ed.*, 43 (2004) 2334.
- 9 J.-H. Liao, T.-J. Lee and C.-T. Su, *Inorg. Chem. Commun.*, 9 (2006) 201.
- 10 H. Park, D. M. Moureau and J. B. Parise, *Chem. Mater.*, 18 (2006) 525.
- 11 L. Huang, H. Wang, J. Chen, Z. Wang, J. Sun, D. Zhao and Y. Yan, *Micropor. Mesopor. Mater.*, 58 (2003) 105.
- 12 T. Ozawa, *Bull. Chem. Soc. Jpn.*, 38 (1965) 1881.
- 13 J. H. Flynn and L. A. Wall, *J. Res. Natl. Bur. Standards*, 70A (1966) 487.
- 14 H. L. Friedman, *J. Polym. Sci. Part C*, 6 (1964) 183.
- 15 S. Vyazovkin, *J. Comput. Chem.*, 22 (2001) 178.
- 16 A. W. Coats and J. P. Redfern, *Nature*, 201 (1964) 68.
- 17 A. W. Coats and J. P. Redfern, *J. Polym. Sci. B, Polym. Lett.*, 3 (1965) 917.
- 18 B. N. Achar, *J. Proc. Int. Clay Conf.*, 1 (1969) 6.
- 19 D. Zhou, E. A. Schmitt, G. G. Z. Zhang, D. Law, C. A. Wight, S. Vyazovkin and D. J. W. Grant, *J. Pharm. Sci.*, 91 (2003) 1367.
- 20 S. Vyazovkin, *J. Therm. Anal. Cal.*, 83 (2006) 45.

Received: April 3, 2007

Accepted: April 5, 2007

OnlineFirst: July 12, 2007

DOI: 10.1007/s10973-007-8494-9